Scalable Polymeric Few-Nanometer Organosilica Membranes with Hydrothermal Stability for Selective Hydrogen Separation

Lingxiang Zhu,‡[1,2,3] Liang Huang,‡[1] Surendar R. Venna,[2,3] Adrienne Blevins,[4] Yifu Ding,[4] David P. Hopkinson,[2] Mark T. Swihart,[1] and Haiqing Lin[1]*

[1] Department of Chemical and Biological Engineering, University at Buffalo, The State University of New York, Buffalo, NY 14260, USA

[2] U.S. Department of Energy, National Energy Technology Laboratory, 626 Cochrans Mill Road, P.O. Box 10940, Pittsburgh, PA 15236, USA

[3] NETL Support Contractor, 626 Cochrans Mill Road, P.O. Box 10940, Pittsburgh, PA 15236, USA

[4] Membrane Science, Engineering and Technology (MAST) Center, Paul M. Rady Mechanical Engineering, University of Colorado at Boulder, Boulder, CO 80309, USA

‡ These authors contributed equally to this work.

* Corresponding author: haiqingl@buffalo.edu (H.L.)

ABSTRACT

Nanoporous silica membranes exhibit excellent H_2/CO_2 separation properties for sustainable H2 production and CO2 capture but are prepared via complicated thermal processes above 400 °C, which prevent their scalable production at a low cost. Here, we demonstrate the rapid fabrication (within 2 min) of ultrathin silica-like membranes (~3 nm) via an oxygen plasma treatment of polydimethylsiloxane-based thin-film composite membranes at 20 °C. The resulting organosilica membranes unexpectedly exhibit H2 permeance of 280–930 GPU (1 GPU = 3.347 × 10–10 mol m^{-2} s^{-1} Pa^{-1}) and H2/CO2 selectivity of 93–32 at 200 °C, far surpassing state-of-the-art membranes and Robeson's upper bound for H_2/CO_2 separation. When challenged with a 3 d simulated syngas test containing water vapor at 200 °C and a 340 d stability test, the membrane shows durable separation performance and excellent hydrothermal stability. The robust H_2/CO_2 separation properties coupled with excellent scalability demonstrate the great potential of these organosilica membranes for economic H_2 production with minimal carbon emissions.

KEYWORDS: silica membranes, CO_2 capture, hydrogen purification, oxygen plasma, polydimethylsiloxane, H_2/CO_2 separation

Blue hydrogen (H_2) as a zero-emission energy carrier has the potential to achieve a large-scale reduction of CO_2 emissions and foster a transition to a carbon-neutral economy.[1-4] H_2 is predominantly produced by steam reforming of natural gas or gasification of coal, processes from which byproduct CO_2 must be captured for utilization or storage to mitigate its emissions to the environment. The state-of-the-art CO_2 capture technology (*e.g.*, the Selexol process) is expensive and may increase the cost of H_2 production by 30%.[5] Gas separation membranes with H_2/CO_2 selectivity of 30 or above at syngas processing temperatures (150 °C or above) would provide a low-cost and energy-efficient alternative for the sustainable production of blue H_2.[6] Industrial gas separation membranes are usually made of polymers with excellent processability and scalability. However, polymers are subject to an inherent permeability/selectivity trade-off, *i.e.*, polymers with higher H_2 permeability tend to have higher free volume and thus lower H_2/CO_2 selectivity.[7-9] Most polymeric membranes also lose size-sieving ability at high temperatures and show low selectivity.

Porous materials with well-controlled ultramicropores with molecular sieving ability have been extensively explored for H_2/CO_2 separation, including silica,[10-12] zeolites,[1, 13] metal-organic frameworks (MOFs),[14] porous organic frameworks,[15] and 2D materials with subnanometer channels[16] such as graphene oxide (GO),[2, 3] MoS_2,[17] graphitic carbon nitride (g-C_3N_4),[18] and ionic covalent organic nanosheets (iCONs).[19] Inorganic nanofillers have been incorporated into polymers to form mixed matrix materials (MMMs) to achieve superior separation properties with improved processability.[20-22] However, the production of defect-free membranes on a large scale presents an enormous challenge. Polymers can also be pyrolyzed at 500 – 900 °C to prepare carbon molecular sieves (CMS)[23] or silica membranes[24, 25] to achieve superior H_2/CO_2 separation properties. However, their production at a commercial scale is energy-intensive and has yet to be demonstrated. For instance, conventional silica membranes show exceptional H_2/CO_2 selectivity

of as high as 100,[10] and they are primarily made from organic precursors (such as tetraethoxysilane and tetramethoxysilane) *via* sol-gel deposition (requiring a calcination step at 400 – 600 °C[10, 26]) or chemical vapor deposition (requiring decomposition of silanes at 500 – 600 °C[27]). Such steps are energy-intensive and require thermally stable ceramic substrates (*e.g.*, porous alumina), making them expensive and non-scalable for industrial production.[10]

Herein, we present a concept of designing membranes by combining the performance of silica membranes with the excellent processability of practical polymeric membranes. Specifically, we prepare polymeric organosilica (POSi) membranes comprising a few-nanometer silica-like film on top of a polydimethylsiloxane (PDMS) based thin-film composite (TFC) membrane (Figure 1a). The membranes are formed by oxygen plasma treatment of the PDMS film at 20 °C and demonstrate H_2/CO_2 selectivity of as high as 100, matching that of conventional silica membranes.[10] The PDMS TFC membrane provides excellent mechanical properties and easy handling, similar to existing industrial gas separation membranes. More importantly, conventional silica membranes have poor hydrothermal stability for practical applications because their hydrophilic nanopores tend to collapse or degrade in the presence of water vapor, especially at high temperatures.[10, 28-30] Numerous efforts such as improving surface hydrophobicity,[31] metal doping,[29, 30] and formation of hybrid inorganic and organic silica[30, 32, 33] have been explored to improving hydrothermal stability, which, however, decreased H_2/CO_2 selectivity. By contrast, our POSi membranes exhibit great hydrothermal stability, along with excellent processability, rendering them the potential for practical H_2/CO_2 separation.

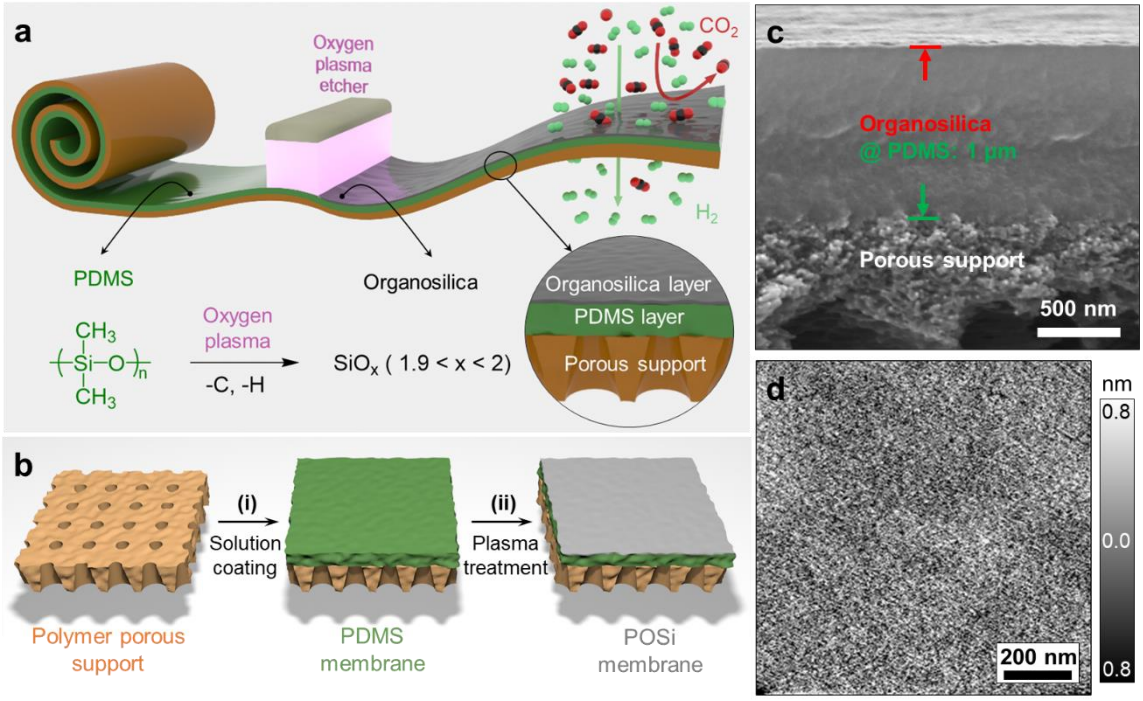

Figure 1. Preparation of POSi membranes. (a) Schematic illustration of a room-temperature approach to silica membranes by integrating oxygen plasma treatment into a conventional polymer membrane fabrication route. Oxygen plasma can convert the surface of the PDMS into a silica-like structure,[29, 30] or organosilica. (b) A schematic of the POSi membrane fabrication procedure, including PDMS coating and plasma treatment. (c) Cross-sectional micrograph of a POSi120 membrane. (d) AFM topographic image showing the surface roughness of a POSi120 membrane.

Oxygen plasma treatment of PDMS has been employed to increase its surface energy and thus wettability for the applications such as microfluidics, implantable prostheses, and soft lithography.[34-36] The oxygen plasma can break organic bonds and remove C and H in the form of H_2O, CO_2, and low molecular weight hydrocarbons, leaving a significant fraction of Si bonded to three or four oxygen atoms on the surface and forming a dense silica-like layer (or organosilica). Plasma modification of PDMS using Ar, N_2, O_2, and NH_3 has also been explored to influence gas

separation properties.[35, 37, 38] Plasma treatment can cross-link PDMS and improve its size-sieving ability. For example, oxygen-plasma treatment of a PDMS film decreased CO_2 permeance from 840 GPU (1 GPU = 3.347×10^{-10} mol m^{-2} s^{-1} Pa^{-1}) to 240 GPU and increased CO_2/CH_4 selectivity from 4.8 to 45 at 25 °C.[39] Argon plasma treatment of PDMS decreased O_2 permeance from 16.7 to 1.5 GPU and increased O_2/N_2 selectivity from 2.4 to 4.6 at 30 °C.[40] Surprisingly, the potential of the PDMS to form silica membranes for high-temperature H_2/CO_2 separation has not previously been recognized.

RESULTS AND DISCUSSION

Membrane fabrication and characterizations. As illustrated in Figure 1a, our approach to scalable silica membranes is built upon a conventional polymer membrane fabrication route integrated with an oxygen plasma treatment. Figure 1b shows the preparation steps for the POSi membranes at 20 °C. A submicron PDMS coating is first applied on top of a porous polybenzimidazole (PBI) support (Figure S1) to form a TFC membrane, which is stable at 200 °C because of the excellent thermal stability of PBI and PDMS.[22] Oxygen plasma is then applied to produce an ultrathin silica-like layer on the PDMS surface, following the simplified reaction scheme shown in Figure 1a. The plasma is ignited in an oxygen flow at 20 °C, and the exposure time is varied from 15 to 360 s to achieve different POSi membrane structures. The obtained samples are denoted as POSi*x*, where *x* is the plasma exposure time in seconds. Figure 1c displays a cross-sectional scanning electron microscopy (SEM) image of a POSi120 membrane, where a porous support is overlaid with a 1 µm-thick PDMS and dense silica-like film. The silica-like layer is too thin to be distinguished from PDMS in the SEM image. As confirmed in-depth profiles discussed below, the silica-like layer gradually transitions to the unmodified PDMS. Such a graded

thin film offers mechanical robustness by eliminating the mechanically weak interface present in typical bilayer configurations. The surface roughness of the plasma-treated PDMS was investigated by atomic force microscopy (AFM). The formation of the silica-like layer does not increase the surface roughness (Figure S2a,b). POSi120 exhibits a smooth surface with a roughness of 0.8 nm (Figure 1d).

Figure 2a presents the reaction occurring on a PDMS surface in the presence of oxygen plasma species like O^+, O^-, O, O_2, and O_3, as validated using X-ray photoelectron spectroscopy (XPS).[36, 37, 39, 41] To avoid interference from the porous substrate, PDMS films of 1 µm were coated on Si wafers and then exposed to the same oxygen plasma condition used for preparing POSi membranes. Increasing the plasma exposure time from 0 to 360 s increases the O/Si ratio, decreases the C/Si ratio, and has no effect on the Si content (25 - 27 mol %, Figure 2b), confirming the oxidation and methyl scission reactions on PDMS and formation of silicons bonded to two ($Si(-O)_2$), three ($Si(-O)_3$), or four oxygen atoms ($Si(-O)_4$ or SiO_2). Noticeably, oxygen plasma drastically changes the chemical compositions of the PDMS surface within 120 s. For instance, the C/Si ratios are 2.0, 1.1, and 0.76 at an exposure time of 0, 15, and 120 s, respectively. Meanwhile, the O/Si ratios of PDMS, POSi15, and POSi120 are 1.0, 1.7, and 1.9, respectively. This oxygen plasma treatment is so efficient that the O/Si and C/Si ratios become stable after 120 s treatment. For example, an additional 240 s exposure only decreases the C/Si ratio by 0.07 and increases the O/Si by 0.1. Consequently, POSi360 possesses a C/Si of 0.69 and an O/Si ratio of 2.0. The high O/Si ratio of 2.0 indicates the PDMS surface is converted to a silica-like structure, which is further confirmed by the XPS peak deconvolution (*cf.* Figure 2c and Table S1).

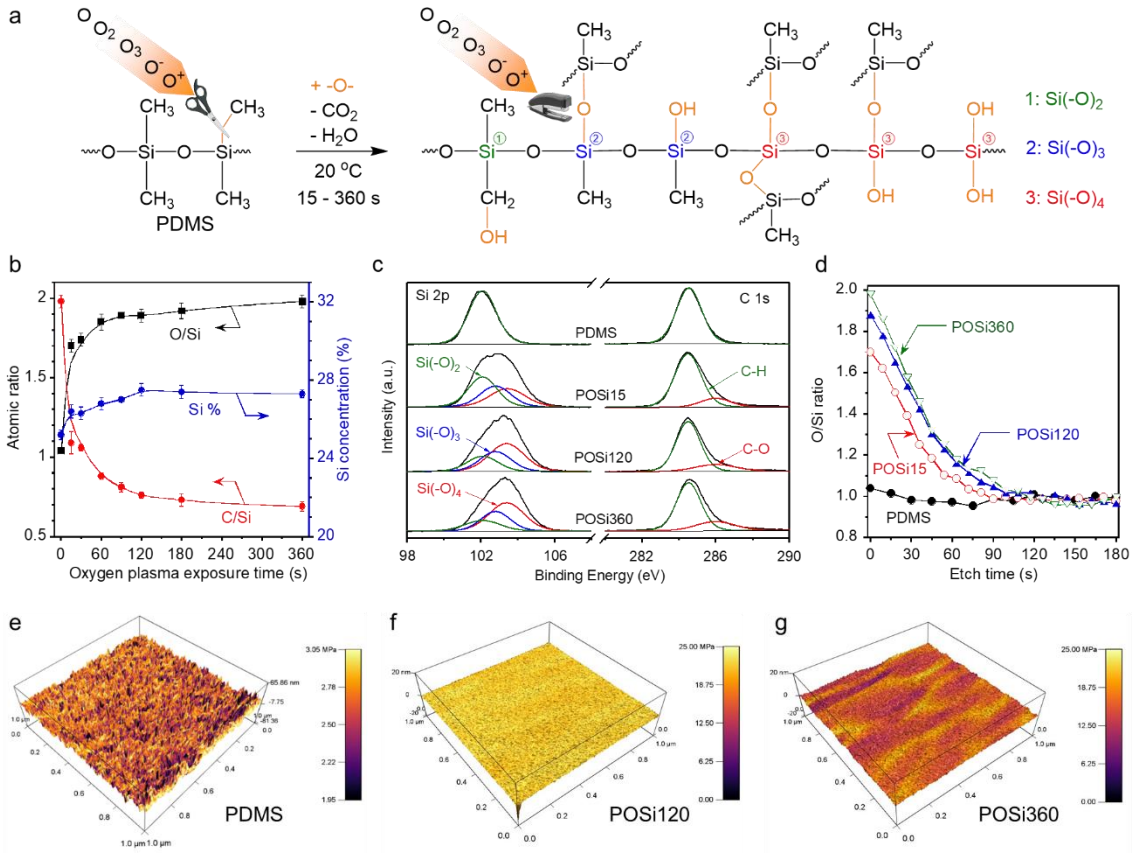

Figure 2. Formation and structure of ultrathin organosilica. (a) Simplified mechanism of oxidation and cross-linking of PDMS by oxygen plasma. (b) The effect of oxygen plasma exposure time on Si concentration and C/Si and O/Si ratios at the PDMS surface. (c) Resolved surface XPS spectra of Si 2p and C 1s peaks and (d) O/Si ratio as a function of argon sputtering etch time of the PDMS and POSi samples. (e-g) AFM mapping of both surface topography (Z-axis of the 3D image) and nanoscale modulus (color map with the scale bars presented on the right) for PDMS, POSi120, and POSi360 surfaces.

Figure 2c compares Si 2p XPS spectra of the pristine PDMS and representative POSi samples. PDMS displays one characteristic peak at 102.1 eV, corresponding to Si bonded to two oxygens.[37] By contrast, the complex Si 2p peaks of POSi can be resolved into three components: $Si(-O)_2$ at

102.1 eV, ($Si(-O)_3$) at 102.8 eV, and SiO_2 at 103.4 eV.[37] The amplitudes of the different Si peaks vary with the plasma exposure time. For example, increasing the plasma exposure time decreases the amplitude of $Si(-O)_2$ peak but significantly increases SiO_2 peak intensity. Table S1 summarizes the Si distribution among different chemical states obtained by deconvolution of those Si 2p peaks. For instance, POSi120 has 12.5 mol% $Si(-O)_2$, 25.3 mol% $Si(-O)_3$, and 62.2 mol% SiO_2, indicating that the oxygen plasma converts the PDMS chains to a silica-like structure on the surface. Figure 2c also compares the resolved C 1s XPS spectra of the PDMS and POSi samples. The PDMS surface presents only a C-H bond at 284.6 eV. By contrast, the POSi samples exhibit both C-H and C-O (at 286.0 eV) bonds, confirming the oxidation of the pendant methyl ($-CH_3$) groups and the formation of hydroxyl groups (C-O-H). Increasing the plasma exposure time from 0 to 120 s substantially increases the C-O content from 0 to 20.2% (Table S1). Figure S3 shows that the peak of Si-O shifts from 532.2 eV for PDMS to 532.8 eV for the POSi samples, confirming the formation of the silanol groups (Si-O-H) after plasma treatment.[42, 43] The formation of the hydroxyl and silanol groups is also evidenced by the decrease of water contact angle from 97° for PDMS to 22° for POSi120 (Figure S4).

Small oxygen plasma species like O^+, O^- and O have a size of ~1.2 Å and can easily diffuse in PDMS and subsequently modify the sub-surface PDMS. The resulting organosilica layers were reported to have thickness varying from 4.5 to 160 nm depending on the power of plasma generator and the exposure time.[37, 38] The POSi structure created in this study is extremely thin as evidenced by its transparency to X-ray diffraction (XRD), Raman and Fourier-transform infrared (FTIR) spectroscopy, as shown in Figure S5a-e. XPS depth profiling combined with argon sputtering was employed to determine the thickness of the organosilica layer in the POSi samples. During the depth profiling, argon sputtering with a fixed time interval was applied to mill away a thin layer

of the specimen surface, and then the XPS detector analyzed the newly exposed surface after each sputtering. More than 20 cycles were repeated for each specimen. Figure 2d plots the O/Si ratio as a function of the argon sputtering etch time. PDMS shows the O/Si ratio of 1.00 ± 0.02, consistent with its theoretical O/Si ratio of 1, and any O/Si ratio over 1 indicates the presence of the oxidized PDMS. The O/Si ratio of the POSi samples decreases with increasing etch time, from a range of 1.7 – 2.0 to a value of 1.0 at 108 s and beyond. Given that POSi is a mixture of silicons bonded to two oxygens ($Si(-O)_2$ or PDMS), three oxygens ($Si(-O)_3$), and four oxygens ($Si(-O)_4$ or SiO_2), a dynamic etching rate depending on the local O/Si ratio (n) of the POSi structure being milled is developed to calculate the organosilica layer thickness. Since the etching rates calibrated for the softest PDMS (O/Si = 1) and hardest SiO_2 in POSi are 0.233 and 0.085 nm/s, respectively, the dynamic etching rate can be expressed as $-0.148n + 0.381$ (nm/s) assuming it decreases linearly with increasing O/Si ratio. Table S2 summarizes the calculated cumulative etching depth at a given etch time. All the POSi samples reach to O/Si ratio of 1.0 at an etching depth less than 20 nm, indicating the plasma treatment only affects the <20 nm-thick PDMS layer. Within the oxidized PDMS, the dense structure with an O/Si ratio greater than 1.5 would primarily perform the molecular sieving for gas separation, because an O/Si ratio of 1.5 indicates that, on average, each Si atom is linked to another three Si atoms to achieve a fully cross-linked structure. Therefore, the highly densified PDMS or silica-like layer was determined to be *ca.* 2.4, 3.2, and 4.2 nm for POSi15, POSi120, and POSi360, respectively (Table S2).

The effect of plasma treatment on nanoscale mechanical properties of PDMS was examined by AFM in a fast-force mapping mode. The pristine PDMS is soft and only shows an elastic modulus of 2.5 ± 0.5 MPa (Figure 2e), similar to its bulk modulus (2.6 MPa).[44] By contrast, the elastic modulus of POSi120 increases to 22 ± 1 MPa (Figure 2f), almost one order magnitude

higher than that of PDMS due to the formation of a silica-like layer. The elastic modulus of POSi360 is also higher than the pristine PDMS but shows a non-uniform surface in terms of a large modulus range of 10 – 25 MPa (Figure 2g), which can be ascribed to topographic convolution from the wavy surface caused by the high plasma exposure time (Figure S2c,d). Additionally, the measurement tends to underestimate the true modulus because AFM indentation depth is on the order of 100 nm, so the stress fields from the AFM tip extend considerably beyond the ultrathin organosilica layer.

Gas transport properties and membrane stability. Figure 3a displays the effect of the oxygen plasma exposure time on H_2/CO_2 separation properties of the POSi membranes when tested with a binary gas mixture of 50% H_2 and 50% CO_2 at 150 °C and 6.9 bar. The POSi membranes were prepared from the TFC membranes with 1 µm-thick PDMS. Increasing the plasma exposure time decreases the mixed-gas permeance but significantly enhances H_2/CO_2 selectivity. For example, POSi15 shows H_2/CO_2 selectivity of 7.2, while POSi360 exhibits a much higher selectivity of 100, comparable to that (98) of a calcined silica membrane operated at 300 °C.[10] By contrast, the pristine PDMS exhibits H_2/CO_2 selectivity of only 0.25 at 35 °C (Table S3) and 1.2 at 150 °C.[45] Increasing the plasma treatment time from 15 to 360 s decreases the H_2 permeance from 930 to 54 GPU at 150 °C. We have also compared gas permeance of POSi15 (the most permeable sample among the POSi samples) with that of the pristine PDMS at 35 °C. PDMS and POSi15 exhibit H_2 permeance of 570 ± 20 GPU and 28 ± 1 GPU at 35 °C, respectively, indicating a negligible transport resistance in the PDMS layer compared with the organosilica layer.

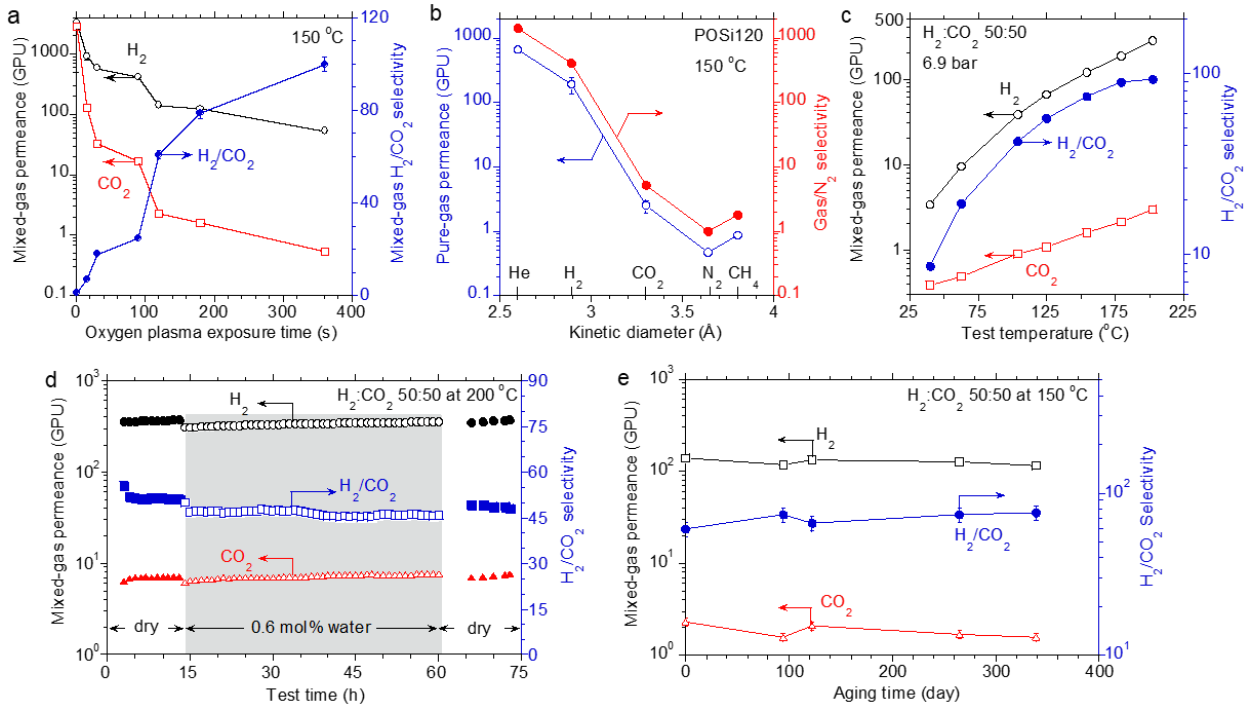

Figure 3. Gas separation properties of the POSi120 membranes at 150 °C unless specified. (a) Effect of oxygen plasma exposure time on the mixed-gas separation performance. (b) Pure-gas permeance and gas/N_2 selectivity of a POSi120 membrane. (c) Effect of test temperature on the mixed-gas permeance and selectivity of a POSi120 membrane. (d) Stability test in a POSi120 membrane using H_2:CO_2 (50:50) with and without water vapor at 200 °C. (e) Long-term stability of POSi120 over 340 days. Error bars are less than 4% of the values unless specified.

POSi120 membrane was chosen for further study because of its balanced mixed-gas H_2 permeance (144 GPU) and H_2/CO_2 selectivity (61) at 150 °C. Figure 3b shows pure-gas permeance at 150 °C to probe pore sizes of the organosilica structure. POSi120 exhibits pure-gas permeance of He (kinetic diameter: 2.6 Å), H_2 (2.89 Å), CO_2 (3.3 Å), N_2 (3.64 Å), and CH_4 (3.8 Å) of 660 ± 30 GPU, 190 ± 7 GPU, 2.5 ± 0.1 GPU, 0.47 ± 0.02 GPU, and 0.86 ± 0.04 GPU, respectively. Gas permeance decreases with increasing penetrant size from 2.6 Å for He to 3.64 Å for N_2, suggesting

that the gas permeation follows a molecular sieving mechanism. However, CH_4 has slightly higher permeance than N_2, though CH_4 (3.8 Å) has a larger kinetic diameter than N_2 (3.64 Å). Similar phenomena have been reported for other molecular-sieving membranes, such as graphene oxide membranes,[2, 3] though the reason is still unclear. Figure 3b shows that the gas/N_2 selectivity decreases with increasing gas molecular size. For example, the membrane shows H_2/N_2 and CO_2/N_2 selectivity of 410 and 8.3, respectively. The sharp decrease suggests that most of the nanopores have sizes between H_2 (2.89 Å) and CO_2 (3.3 Å). POSi120 membrane also shows H_2O/H_2 selectivity of 2.7 when challenged with a binary mixture, which can be ascribed to the smaller kinetic diameter but the higher critical temperature of H_2O than H_2.

Figure 3c shows that increasing the temperature drastically increases mixed-gas H_2 permeance and H_2/CO_2 selectivity. For example, the POSi120 membrane shows H_2 permeance of 3.4 GPU and H_2/CO_2 selectivity of 8.6 at 40 °C, and H_2 permeance of 280 ± 5 GPU and H_2/CO_2 selectivity of 93 ± 1 at 200 °C. By contrast, a calcined silica membrane (Si600) with a comparable thickness (30 nm) showed H_2 permeance of 1490 GPU and H_2/CO_2 selectivity of 71 at 200 °C,[10] indicating that the POSi120 has a more densified structure with stronger size-sieving ability than the calcined silica membrane. The effect of the temperature on gas permeance can be described using the Arrhenius equation with an activation energy of permeation of 33 kJ/mol for H_2 and 15 kJ/mol for CO_2 (Figure S6). The lower activation energy of permeation for CO_2 can be ascribed to its greater enthalpy of condensation than H_2.[24, 45] This phenomenon agrees well with that observed in silica membranes supported on alumina.[10, 26]

Industrial syngas contains small amounts of other components such as H_2O.[8, 22] Figure 3d shows the effect of water vapor on mixed-gas separation properties and stability of a POSi120 membrane at 6.9 bar and 200 °C. The membrane was initially tested using a dry gas mixture (50%

H_2/50% CO_2) for 13 h. Then 0.6 mol% water vapor (with a partial pressure of 0.041 bar) was introduced in the mixed-gas feed for a continuous test of 47 h. The water vapor content is lower than that in the syngas, but it provides a useful indication of the hydrothermal stability of the membranes. Adding water vapor decreases the mixed-gas H_2 permeance from 370 to 350 GPU and decreases the H_2/CO_2 selectivity from 51 to 46. When the feed gas was switched back to the dry gas, the H_2 permeance and H_2/CO_2 selectivity recovered to 370 GPU and 49, respectively. This 3-day continuous test confirms that the POSi membranes are stable for H_2/CO_2 separation in the presence of the water vapor. Incorporating organic Si–C_xH_y–Si links[32] or –CH_3 groups[33] in silica membranes has been reported to significantly improve the hydrothermal stability of silica membranes and enable their pervaporation applications at high temperatures. The excellent hydrothermal stability of our POSi membranes arises from the residual –CH_3 groups, *i.e.*, 0.61 - CH_3 groups linked to each Si atom in POSi120 as calculated in Table S1 using the C/Si ratio in Figure 2b and the deconvoluted C 1s peaks in Figure 2c. Figure 3e also shows the long-term stability of a POSi120 sample for mixed-gas H_2/CO_2 separation properties. The sample was stored in the air at ~ 23 °C and tested periodically at 150 °C for 340 days, and the aggregate testing time was 215 h. The H_2 permeance decreases by 14%, while the H_2/CO_2 selectivity increases by 27% over this period. Such performance variation for one year is common for industrial membranes. The membrane was further tested at 200 °C for 60 h (Figure S7) and showed stable H_2 permeance of 280 GPU and H_2/CO_2 selectivity of 93. The sample had an overall test of 275 h at 150 - 200 °C, validating its viability for practical applications.

Superior gas separation performance of POSi membranes. Figure 4a shows the effect of the PDMS layer thickness on the mixed-gas H_2/CO_2 separation performance in POSi120 when tested

with a binary mixture of 50:50 H_2/CO_2 at 200 °C. Decreasing the PDMS layer from 1 µm to 200 nm increases the H_2 permeance from 280 to 930 GPU but decreases the H_2/CO_2 selectivity from 93 to 32, which might be ascribed to the extremely small defects (in nanometers) formed during the fabrication for the thin PDMS layer. However, it is impossible to image or quantify these few-nanometer defects. Figure S8a,b shows a 1 µm-thick PDMS layer has smoother surface than a 200-nm thick PDMS layer, and Figure S8c,d displays the cross-sectional SEM images of the membranes with a thinner PDMS layer (200-300 nm). Both PDMS layers seem to be dense without large pinholes. Figure 4a also compares the H_2/CO_2 separation performance of the POSi membranes with the state-of-the-art TFC membranes, including commercial Proteus™ membrane,[6] cross-linked polyamide TFC membranes,[46] PBI hollow fiber membranes,[9] and PBI-based MMMs containing ZIF-8[47] and Pd nanoparticles.[22, 48] All the POSi120 membranes are superior to the polymeric membrane benchmarks in terms of combined high permeance and selectivity and demonstrate their promise for low-cost pre-combustion CO_2 capture and H_2 production.

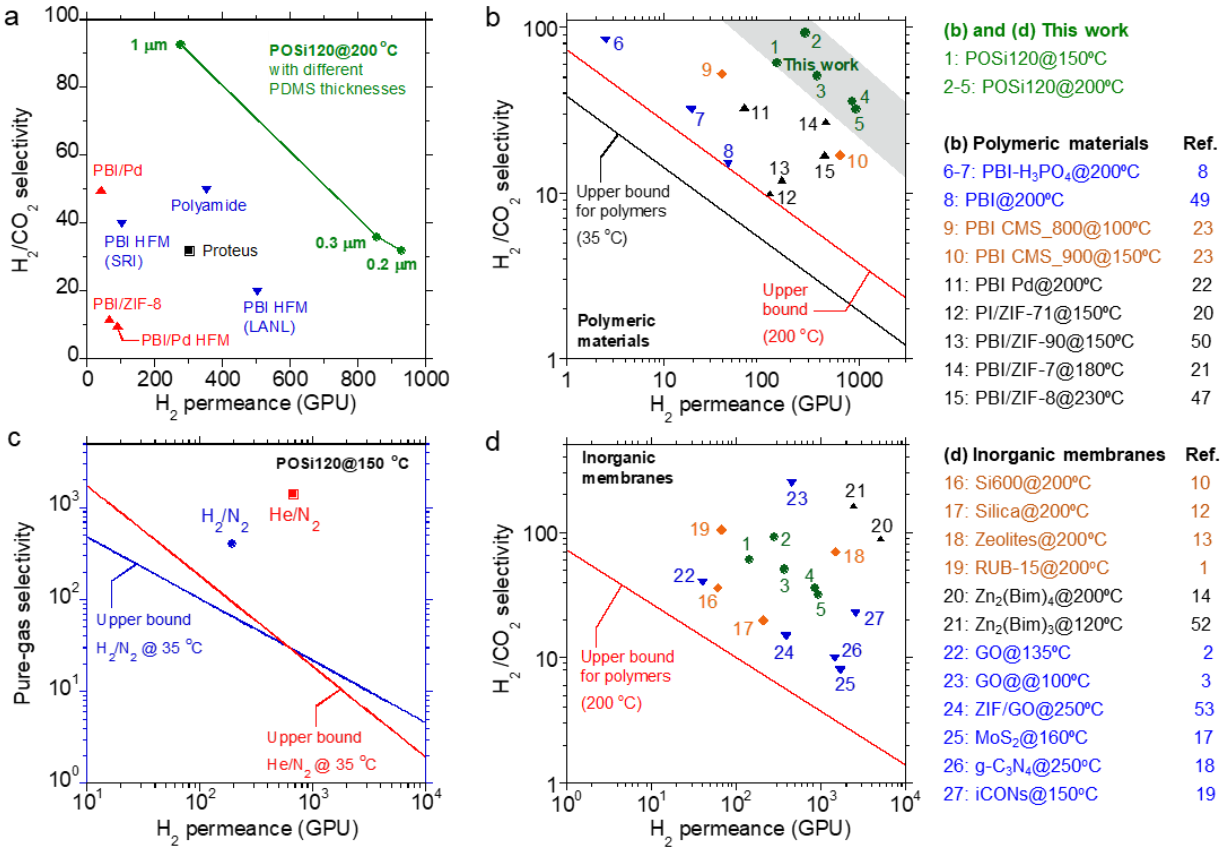

Figure 4. Superior gas separation performance of POSi membranes. (a) Comparison of mixed-gas H_2/CO_2 separation performance of the POSi120 membranes with state-of-the-art membranes, including Proteus™ at 150 °C,[6] polyamides at 140 °C,[46] PBI hollow fiber membranes (HFMs) at 200-250 °C,[9] and MMMs of PBI/Pd at 175 °C[22] and 60 °C,[48] and PBI/ZIF-8 at 180 °C.[47] (b) Comparison with polymeric materials, including PBI,[49] PBI doped with H_3PO_4,[8] CMS,[23] and MMMs[20-22, 47, 50] in the Robeson's upper bound plot.[51] These materials are assumed to be fabricated into 1-μm thick TFC membranes. The black line is the 2008 upper bound at 35 °C, and the red line is the upper bound predicted for 200 °C.[22] (c) Superior H_2/N_2 and He/N_2 separation performance *versus* Robeson's 2008 upper bounds.[51] (d) Comparison with inorganic membranes, including silica,[10, 12] zeolites,[1, 13] MOFs,[14, 52] GO,[2, 3] ZIF/GO,[53] MoS_2,[17] g-C_3N_4 nanosheets,[18] and iCONs.[19] The detailed membrane separation performance is also summarized in Table S4.

Figure 4b compares H_2/CO_2 separation performance of the POSi120 membranes with state-of-the-art polymeric materials (including PBI,[49] PBI/H_3PO_4,[8] CMS,[23] and MMMs[20-22, 47, 50]) in a Robeson's plot.[51] The POSi120 samples for comparison include the membranes prepared from 1 µm PDMS and then evaluated at 150 - 200 °C (Points 1-3) and those fabricated from 200 and 300 nm PDMS and operated at 200 °C (Points 4-5). Polymers with excellent processability have great potential to be fabricated into TFC membranes with an assumed selective layer thickness of 1 µm. The upper bound defines the highest H_2/CO_2 selectivity achievable for any H_2 permeance in polymers[8, 22, 51] and is often used to benchmark any new materials developed. These polymeric materials show the separation properties on or above the upper bound. By contrast, our organosilica materials surpass the upper bounds and the start-of-the-art polymeric materials for H_2/CO_2 separation.

Syngas may contain light gases such as N_2, and thus, the membranes should also have high H_2/N_2 separation properties. Figure 4c compares the POSi120 with state-of-the-art polymers for H_2/N_2 separation.[51] The upper bounds were taken from the literature at ≈35 °C. The POSi120 exhibits separation properties above the upper bound. Figure 4c also suggests that the POSi120 has superior He/N_2 separation properties.

Figure 4d compares the POSi120 membranes with state-of-the-art inorganic membranes for H_2/CO_2 separation such as silica,[10, 12] zeolites,[1, 13] MOFs,[14, 52] GO,[2, 3] ZIF/GO,[53] MoS_2,[17] g-C_3N_4 nanosheets,[18] and iCONs.[19] These inorganic membranes exhibit H_2/CO_2 separation properties above the upper bound (which is defined for polymeric membranes). The POSi120 membranes show competitive separation properties. Several membranes based on 2D materials show better properties than the POSi120, including zeolites,[13] 2D MOFs,[14, 52] and GO.[3] However, unlike the

POSi membranes, these 2D materials-based membranes are faced with a significant challenge of reproducible fabrication on a large scale.

CONCLUSIONS

In summary, we prepare nanoporous silica-like membranes comprising a thin selective layer (≈ 3 nm) on conventional polymeric TFC membranes by oxygen-plasma treatment of PDMS membranes at room temperature. This approach – low-cost surface treatment of a polymeric membrane to create an inorganic selective layer – represents a paradigm shift in approaches to membrane development, bringing together the traditionally disparate spheres of polymeric and inorganic membrane research to combine the strengths of both. Pre-combustion carbon capture is a critical approach to produce blue H_2 while mitigating carbon emissions. The POSi membranes with superior H_2/CO_2 separation properties can be reproducibly prepared from inexpensive polymers without energy-intensive hydrothermal treatment or calcination, dramatically impacting the economics of CO_2 capture for the production of blue H_2 on a large scale with minimal CO_2 release into the atmosphere. The POSi membranes with tunable molecular sieving abilities have promise for other gas and vapor separations as well.

EXPERIMENTAL SECTION

Materials. Celazole® PBI S15 solution with 15 wt. % PBI dissolved in *N*,*N*-dimethylacetamide (DMAc) was provided by PBI Performance Products, Inc. (Charlotte, SC). Anhydrous DMAc (>99.5%), toluene (>99.9%), and poly(ethylene glycol) (PEG, a number average molecular weight of 400 g/mol) were purchased from Thermo Fisher Scientific Company (Waltham, MA). Iso-octane (>99%) was supplied by Sigma-Aldrich Chemical Company (St. Louis, MO). Methanol

(99%) was provided by VWR International Company (Radnor, PA). DEHESIVE® 944 cross-linkable polydimethylsiloxane (PDMS), WACKER® catalyst OL, and WACKER® crosslinker V24 were supplied by Wacker Chemical Corporation, Adrian, MI. Gas cylinders of H_2, He, Ar, N_2, and CO_2 with ultrahigh purity (99.999%) were obtained from Airgas USA, LLC (Buffalo, NY). All chemicals were used as received without further purification.

Fabrication of POSi membranes. POSi membranes were fabricated in three steps, including preparation of a PBI porous support, coating a PDMS layer, and oxygen plasma treatment.

First, the PBI porous support was prepared *via* a phase inversion method.[22] For this, 0.5 g poly(ethylene glycol) (PEG, M_w 400 g/mol) was added to 10 g PBI S15 solution (PBI Performance Products, Inc.) containing 15 wt.% PBI in *N*,*N*-dimethylacetamide (DMAc). Second, 2 mL solution was cast on a 10 × 15 cm stainless steel wire cloth (mesh size: 325 × 2300, McMaster-Carr, OH) using a casting knife with a gate clearance of 200 μm. Third, the liquid film was immersed into a water bath at 50 °C for 1 h to form the porous support, which then went through a solvent exchange in the order of DI water, methanol, and iso-octane at 25 °C for 30 min each. Finally, the PBI support was obtained by drying at 25 °C in a fume hood for 1 day.

Second, the PDMS coating was prepared *via* a dip-coating method. The PBI support was first cut into 3 × 3 cm samples and then masked onto a glass slide using aluminum tape with all edges sealed. The sample was then dipped into a 2.0 wt.% PDMS coating solution for 5 s. After curing at 100 °C for 30 mins, the composite membrane with a PDMS layer of 1 μm can be obtained. The 2 wt.% PDMS coating solution was prepared by dissolving 900 mg Dehesive® 944 (Wacker Chemical Corporation, Adrian, MI, USA), 100 mg Wacker cross-linker V24, and 60 mg Wacker catalyst OL in 43.9 g toluene. Thinner PDMS layers of 200 – 300 nm can be prepared using coating solutions of 0.5 wt% -1.0 wt%.

Finally, the POSi membranes were fabricated by oxygen plasma treatment in a plasma etcher (Trion Technology Oracle III, Clearwater, FL, USA). Figure S9 shows a schematic of the plasma treatment system equipped with an inductively coupled plasma (ICP) radiofrequency generator controlling plasma fluxes and a reactive ion etching (RIE) radiofrequency generator attracting and accelerating the plasma towards the membrane sample. The RIE and ICP power was set at 20 and 50 Watt, respectively, and the oxygen flow rate was 10 cm^3/min at a chamber pressure of 6.7 Pa at 20 °C. Plasma exposure time was varied from 15 to 360 s to achieve different degrees of surface modification.

Characterizations. SEM was performed using a focused ion beam scanning electron microscope (Carl Zeiss AURIGA CrossBeam, German) and FEI Quanta™ 600F scanning electron microscope (Thermo Fisher Scientific, OR, USA). To reduce the charging effect during SEM imaging, a 2 and 12 nm-thick gold-palladium alloy coating was respectively deposited onto the surface and cross-section specimens in a sputter coater (EMS 150TES, Quorum Technologies, East Sussex, UK). Cross-section specimens were prepared *via* a liquid nitrogen freeze-fracturing method. XPS analysis and depth profiling were performed using a PHI 5600ci photoelectron spectrometer with a Mg X-ray source (Physical Electronics Inc., Chanhassen, MN, USA). The analysis area had a diameter of 150 µm (~18,000 μm^2). Sputter depth profiling was performed using 2 kV/20 mA argon ions with a beam diameter of 250 µm. The resulting etching rate was 0.233 and 0.085 nm/s calibrated using PDMS and SiO_2, respectively. AFM was performed using a Cypher atomic force microscope (Asylum Research, Santa Barbara, CA, USA) in Fast Force Mapping mode with an indentation force of 30 nN. The cantilever used (All in One-Al, Budget Sensors, Bulgaria) had a stiffness of 2.36 N/m and a tip radius of 10 nm. The PDMS and POSi samples for XPS and AFM analysis were prepared on Si wafers in the same procedure of fabricating POSi membranes. FT-

IR spectra were collected on a vertex 70 Burker spectrometer (Billerica, MA, US). XRD was performed using a Rigaku Ultima IV diffractometer with Cu Kα radiation (λ = 0.15418 nm, Rigaku, Japan). Raman spectra were collected using Raman spectrometer (Renishaw InVia, UK) with a 514 nm laser source. The water contact angle was measured using a Ramé Hart contact angle goniometer (Model 190, Succasunna, NJ).

Gas permeation measurement. Pure- and mixed-gas permeance at 40 - 200 °C was determined using a constant-pressure and variable-volume apparatus, as illustrated in Figure S10.[49] The membrane was masked using a copper disc (hole diameter: 1 - 2.5 cm) with its rim sealed with Devcon® epoxy (IWT, Hartford, CT, USA). The sample was then loaded into a stainless-steel permeation cell providing countercurrent flows for both feed and sweep gas. The feed gas (H_2, CO_2, or H_2/CO_2 mixture) at 6.9 barg had a flow rate of 200 cm^3 (STP) min^{-1} to achieve a stage-cut less than 1%. Water vapor could be introduced to the feed gas using a bubbler at 25 °C. The humidifier provided 0.041 bar water vapor (or 0.6 mol%) to the gas stream at 6.9 bar. N_2 was used as a sweep gas on the permeate side with a flow rate (S) of 2 - 10 cm^3 (STP) min^{-1} and 1 atm. The composition of the permeate and retentate stream was periodically analyzed using a 3000 Micro GC gas analyzer (Inficon Inc., Syracuse, NY, USA). Gas permeance (P_A/l) of gas component A can be calculated using the following equation:

$$P_A / l = \frac{x_A S}{x_{sweep} A (p_{2,A} - p_{1,A})} \quad \text{(Equation 1)}$$

where A (cm^2) is the active area of the membrane for gas permeation, $p_{2,A}$ and $p_{1,A}$ are the partial pressure of gas component A in the feed and permeate side, respectively, and x_A and x_{sweep} are the mole fraction of gas component A and sweep gas in the sweep-out stream, respectively.

ASSOCIATED CONTENT

Supporting Information

The Supporting Information is available free of charge at https://pubs.acs.org/doi/10.1021/acsnano.1c03492.

Characterizations (SEM, XPS, AFM, Raman, FT-IR, XRD, and water contact angle) of porous PBI support, PDMS coating, and POSi membranes; activation energy determination for H2 and CO2 permeation across a POSi120 membrane, separation performance of a POSi120 membrane after being aged for 340 d, and schematic illustrations of the plasma treatment equipment and gas permeation apparatus. XPS deconvolution results, XPS depth profiling results, gas permeance of PDMS membranes, and detailed H2/CO2 separation properties and testing conditions of the membrane materials selected for comparison in Figure 4 (PDF)

AUTHOR INFORMATION

Corresponding Author

Haiqing Lin - Department of Chemical and Biological Engineering, University at Buffalo, The State University of New York, Buffalo, New York 14260, United States. Email: haiqingl@buffalo.edu

Authors

Lingxiang Zhu - Department of Chemical and Biological Engineering, University at Buffalo, The State University of New York, Buffalo, New York 14260, United States; U.S. Department of Energy, National Energy Technology Laboratory, 626 Cochrans Mill Road, P.O. Box 10940,

Pittsburgh, Pennsylvania 15236, United States; NETL Support Contractor, 626 Cochrans Mill Road, P.O. Box 10940, Pittsburgh, Pennsylvania 15236, United States

Liang Huang - Department of Chemical and Biological Engineering, University at Buffalo, The State University of New York, Buffalo, New York 14260, United States.

Surendar R. Venna - U.S. Department of Energy, National Energy Technology Laboratory, 626 Cochrans Mill Road, P.O. Box 10940, Pittsburgh, Pennsylvania 15236, United States; NETL Support Contractor, 626 Cochrans Mill Road, P.O. Box 10940, Pittsburgh, Pennsylvania 15236, United States

Adrienne K. Blevins - Membrane Science, Engineering and Technology Center, Paul M. Rady Mechanical Engineering, University of Colorado at Boulder, Boulder, Colorado 80309, United States

Yifu Ding - Membrane Science, Engineering and Technology Center, Paul M. Rady Mechanical Engineering, University of Colorado at Boulder, Boulder, Colorado 80309, United States.

David P. Hopkinson - U.S. Department of Energy, National Energy Technology Laboratory, 626 Cochrans Mill Road, P.O. Box 10940, Pittsburgh, Pennsylvania 15236, United States

Mark T. Swihart - Department of Chemical and Biological Engineering, University at Buffalo, The State University of New York, Buffalo, New York 14260, United States

Author Contributions

L.Z. and L.H. contributed equally to this work. H.L., L.Z., and L.H. conceived the approach and conducted the experimental design. L.Z., L.H., S.V., and A.B. fabricated and characterized materials. L.Z., L.H., Y.D., M.T.S., and H.L. performed the data analysis,

and all authors contributed to the discussion of the result. H.L. and D.P.H. supervised the project. The manuscript was written through contributions of all authors. All authors have given approval to the final version of the manuscript.

Notes

The authors declare the following competing financial interest(s): L. Zhu, L. Huang, M. T. Swihart and H. Lin. have filed a U.S. patent application based on this work.

ACKNOWLEDGMENT

This work was supported by the U.S. Department of Energy National Energy Technology Laboratory (Award # DE-FE0026463) and the U.S. National Science Foundation (NSF #1554236). Acknowledgment is made to the Donors of the American Chemical Society Petroleum Research Fund for partial support of this research.

REFERENCES

(1) Dakhchoune, M.; Villalobos, L. F.; Semino, R.; Liu, L. M.; Rezaei, M.; Schouwink, P.; Avalos, C. E.; Baade, P.; Wood, V.; Han, Y.; Ceriotti, M.; Agrawal, K. V. Gas-Sieving Zeolitic Membranes Fabricated by Condensation of Precursor Nanosheets. *Nat. Mater.* **2020,** 20, 362–369.

(2) Kim, H.; Yoon, H.; Yoon, S.; Yoo, B.; Ahn, B.; Cho, Y.; Shin, H.; Yang, H.; Paik, U.; Kwon, S.; Choi, J.; Park, H. Selective Gas Transport through Few-Layered Graphene and Graphene Oxide Membranes. *Science* **2013,** 342, 91-95.

(3) Li, H.; Song, Z.; Zhang, X.; Huang, Y.; Li, S.; Mao, Y.; Ploehn, H. J.; Bao, Y.; Yu, M. Ultrathin, Molecular-Sieving Graphene Oxide Membranes for Selective Hydrogen Separation. *Science* **2013,** 342, 95-98.

(4) Lin, H.; Van Wagner, E.; Freeman, B. D.; Toy, L. G.; Gupta, R. P. Plasticization-Enhanced Hydrogen Purification Using Polymeric Membranes. *Science* **2006,** 311, 639-642.

(5) Miller, D. C.; Litynski, J. T.; Brickett, L. A.; Morreale, B. D. Toward Transformational Carbon Capture Systems. *AIChE J.* **2016,** 62, 2-10.

(6) Merkel, T. C.; Zhou, M.; Baker, R. W. Carbon Dioxide Capture with Membranes at an IGCC Power Plant. *J. Membr. Sci.* **2012,** 389, 441-450.

(7) Bilchak, C. R.; Jhalaria, M.; Huang, Y.; Abbas, Z.; Midya, J.; Benedetti, F. M.; Parisi, D.; Egger, W.; Dickmann, M.; Minelli, M.; Doghieri, F.; Nikoubashman, A.; Durning, C. J.; Vlassopoulos, D.; Jestin, J.; Smith, Z. P.; Benicewicz, B. C.; Rubinstein, M.; Leibler, L.; Kumar, S. K. Tuning Selectivities in Gas Separation Membranes Based on Polymer-Grafted Nanoparticles. *ACS Nano* **2020,** 14, 17174-17183.

(8) Zhu, L.; Swihart, M. T.; Lin, H. Unprecedented Size-Sieving Ability in Polybenzimidazole Doped with Polyprotic Acids for Membrane H_2/CO_2 Separation. *Energy Environ. Sci.* **2018,** 11, 94-100.

(9) Hu, L.; Pal, S.; Nguyen, H.; Bui, V.; Lin, H. Molecularly Engineering Polymeric Membranes for H_2/CO_2 Separation at 100-300 °C. *J. Polym. Sci.* **2020,** 58, 2467-2481.

(10) de Vos, R. M.; Verweij, H. High-Selectivity, High-Flux Silica Membranes for Gas Separation. *Science* **1998,** 279, 1710-1711.

(11) Yacou, C.; Smart, S.; da Costa, J. C. D. Long Term Performance Cobalt Oxide Silica Membrane Module for High Temperature H_2 Separation. *Energy Environ. Sci.* **2012,** 5, 5820-5832.

(12) Song, H.; Wei, Y.; Qi, H. Tailoring Pore Structures to Improve the Permselectivity of Organosilica Membranes by Tuning Calcination Parameters. *J. Mater. Chem. A* **2017,** 5, 24657-24666.

(13) Yu, M.; Funke, H. H.; Noble, R. D.; Falconer, J. L. H_2 Separation Using Defect-Free, Inorganic Composite Membranes. *J. Am. Chem. Soc.* **2011,** 133, 1748-1750.

(14) Peng, Y.; Li, Y.; Ban, Y.; Jin, H.; Jiao, W.; Liu, X.; Yang, W. Metal-Organic Framework Nanosheets as Building Blocks for Molecular Sieving Membranes. *Science* **2014,** 346, 1356-1359.

(15) Shan, M.; Liu, X.; Wang, X.; Yarulina, I.; Seoane, B.; Kapteijn, F.; Gascon, J. Facile Manufacture of Porous Organic Framework Membranes for Precombustion CO_2 Capture. *Sci. Adv.* **2018,** 4, eaau1698.

(16) Shen, J.; Liu, G.; Huang, K.; Chu, Z.; Jin, W.; Xu, N. Subnanometer Two-Dimensional Graphene Oxide Channels for Ultrafast Gas Sieving. *ACS Nano* **2016,** 10, 3398-409.

(17) Achari, A.; Sahana, S.; Eswaramoorthy, M. High Performance MoS_2 Membranes: Effects of Thermally Driven Phase Transition on CO_2 Separation Efficiency. *Energy Environ. Sci.* **2016,** 9, 1224-1228.

(18) Villalobos, L. F.; Vandat, M. T.; Khchoune, M.; Nadizadeh, Z.; Mensi, M.; Oveisi, E.; Campi, D.; Marzari, N.; Agrawal, K. V. Large-Scale Synthesis of Crystalline G-C_3N_4 Nanosheets and High-Temperature H_2 Sieving from Assembled Films. *Sci. Adv.* **2020,** 6, eaay9851.

(19) Ying, Y.; Tong, M.; Ning, S.; Ravi, S. K.; Peh, S. B.; Tan, S. C.; Pennycook, S. J.; Zhao, D. Ultrathin Two-Dimensional Membranes Assembled by Ionic Covalent Organic Nanosheets with Reduced Apertures for Gas Separation. *J. Am. Chem. Soc.* **2020,** 142, 4472-4480.

(20) Japip, S.; Liao, K.; Chung, T. Molecularly Tuned Free Volume of Vapor Cross-Linked 6FDA-Durene/ZIF-71 MMMs for H_2/CO_2 Separation at 150 °C. *Adv. Mater.* **2016,** 29, 1603833.

(21) Yang, T.; Xiao, Y.; Chung, T. Poly-/Metal-Benzimidazole Nano-Composite Membranes for Hydrogen Purification. *Energy Environ. Sci.* **2011,** 4, 4171-4180.

(22) Zhu, L.; Yin, D.; Qin, Y.; Konda, S.; Zhang, S.; Zhu, A.; Liu, S.; Xu, T.; Swihart, M. T.; Lin, H. Sorption-Enhanced Mixed Matrix Membranes with Facilitated Hydrogen Transport for Hydrogen Purification and CO_2 Capture. *Adv. Funct. Mater.* **2019,** 29, 1904357.

(23) Omidvar, M.; Nguyen, H.; Huang, L.; Doherty, C. M.; Hill, A. J.; Stafford, C. M.; Feng, X.; Swihart, M. T.; Lin, H. Unexpectedly Strong Size-Sieving Ability in Carbonized Polybenzimidazole for Membrane H_2/CO_2 Separation. *ACS Appl. Mater. Interfaces* **2019,** 11, 47365-47372.

(24) Adams, J.; Bighane, N.; Koros, W. J. Pore Morphology and Temperature Dependence of Gas Transport Properties of Silica Membranes Derived from Oxidative Thermolysis of Polydimethylsiloxane. *J. Membr. Sci.* **2017,** 524, 585-595.

(25) Nguyen, B.; Dabir, S.; Tsotsis, T.; Gupta, M. Fabrication of Hydrogen-Selective Silica Membranes *via* Pyrolysis of Vapor Deposited Polymer Films. *Ind. Eng. Chem. Res.* **2019,** 58, 15190-15198.

(26) de Vos, R. M.; Verweij, H. Improved Performance of Silica Membranes for Gas Separation. *J. Membr. Sci.* **1998,** 143, 37-51.

(27) Nomura, M.; Yamaguchi, T.; Nakao, S. Silicalite Membranes Modified by Counterdiffusion CVD Technique. *Ind. Eng. Chem. Res.* **1997,** 36, 4217-4223.

(28) Duke, M. C.; da Costa, J. C. D.; Do, D. D.; Gray, P. G.; Lu, G. Q. Hydrothermally Robust Molecular Sieve Silica for Wet Gas Separation. *Adv. Funct. Mater.* **2006,** 16, 1215-1220.

(29) Song, H.; Zhao, S.; Lei, J.; Wang, C.; Qi, H. Pd-Doped Organosilica Membrane with Enhanced Gas Permeability and Hydrothermal Stability for Gas Separation. *J. Mater. Sci.* **2016,** 51, 6275-6286.

(30) ten Hove, M.; Luiten-Olieman, M. W. J.; Huiskes, C.; Nijmeijer, A.; Winnubst, L. Hydrothermal Stability of Silica, Hybrid Silica and Zr-Doped Hybrid Silica Membranes. *Sep. Purif. Technol.* **2017,** 189, 48-53.

(31) Wei, Q.; Wang, Y.-L.; Nie, Z.-R.; Yu, C.-X.; Li, Q.-Y.; Zou, J.-X.; Li, C.-J. Facile Synthesis of Hydrophobic Microporous Silica Membranes and Their Resistance to Humid Atmosphere. *Microporous Mesoporous Mater.* **2008,** 111, 97-103.

(32) Castricum, H. L.; Sah, A.; Kreiter, R.; Blank, D. H. A.; Vente, J. F.; ten Elshof, J. E. Hybrid Ceramic Nanosieves: Stabilizing Nanopores with Organic Links. *Chem. Commun.* **2008**, 1103-1105.

(33) Campaniello, J.; Engelen, C. W.; Haije, W. G.; Pex, P. P.; Vente, J. F. Long-Term Pervaporation Performance of Microporous Methylated Silica Membranes. *Chem. Commun.* **2004**, 834-5.

(34) Bhattacharya, S.; Datta, A.; Berg, J. M.; Gangopadhyay, S. Studies on Surface Wettability of Poly(dimethyl) Siloxane (PDMS) and Glass under Oxygen-Plasma Treatment and Correlation with Bond Strength. *J Microelectromech. Syst.* **2005,** 14, 590-597.

(35) Ferguson, G. S.; Chaudhury, M. K.; Sigal, G. B.; Whitesides, G. M. Contact Adhesion of Thin Gold Films on Elastomeric Supports: Cold Welding under Ambient Conditions. *Science* **1991,** 253, 776-778.

(36) Owen, M. J.; Smith, P. J. Plasma Treatment of Polydimethylsiloxane. *J Adhes. Sci. Technol.* **1994,** 8, 1063-1075.

(37) Hillborg, H.; Ankner, J. F.; Gedde, U. W.; Smith, G. D.; Yasuda, H. K.; Wikström, K. Crosslinked Polydimethylsiloxane Exposed to Oxygen Plasma Studied by Neutron Reflectometry and Other Surface Specific Techniques. *Polymer* **2000,** 41, 6851-6863.

(38) Béfahy, S.; Lipnik, P.; Pardoen, T.; Nascimento, C.; Patris, B.; Bertrand, P.; Yunus, S. Thickness and Elastic Modulus of Plasma Treated PDMS Silica-Like Surface Layer. *Langmuir* **2010,** 26, 3372-3375.

(39) Matsuyama, H.; Teramoto, M.; Hirai, K. Effect of Plasma Treatment on CO_2 Permeability and Selectivity of Poly(dimethylsiloxane) Membrane. *J. Membr. Sci.* **1995,** 99, 139-147.

(40) Kramer, P. W.; Yeh, Y. S.; Yasuda, H. Low Temperature Plasma for the Preparation of Separation Membranes. *J. Membr. Sci.* **1989,** 46, 1-28.

(41) Morra, M.; Occhiello, E.; Marola, R.; Garbassi, F.; Humphrey, P.; Johnson, D. On the Aging of Oxygen Plasma-Treated Polydimethylsiloxane Surfaces. *J. Colloid Interface Sci.* **1990,** 137, 11-24.

(42) Paparazzo, E.; Fanfoni, M.; Severini, E.; Priori, S. Evidence of Si–OH Species at the Surface of Aged Silica. *J. Vac. Sci. Tech. A* **1992,** 10, 2892-2896.

(43) Briggs, D.; Beamson, G. XPS Studies of the Oxygen 1s and 2s Levels in a Wide Range of Functional Polymers. *Anal. Chem.* **1993,** 65, 1517-1523.

(44) Wang, Z.; Volinsky, A. A.; Gallant, N. D. Crosslinking Effect on Polydimethylsiloxane Elastic Modulus Measured by Custom-Built Compression Instrument. *J. Appl. Polym. Sci.* **2014,** 131, 41050.

(45) Merkel, T. C.; Gupta, R. P.; Turk, B. S.; Freeman, B. D. Mixed-Gas Permeation of Syngas Components in Poly(dimethylsiloxane) and Poly(1-Trimethylsilyl-1-Propyne) at Elevated Temperatures. *J. Membr. Sci.* **2001,** 191, 85-94.

(46) Ali, Z.; Pacheco, F.; Litwiller, E.; Wang, Y.; Han, Y.; Pinnau, I. Ultra-Selective Defect-Free Interfacially Polymerized Molecular Sieve Thin-Film Composite Membranes for H_2 Purification. *J. Mater. Chem. A* **2018,** 6, 30-35.

(47) Yang, T.; Shi, G.; Chung, T. Symmetric and Asymmetric Zeolitic Imidazolate Frameworks (ZIFs)/Polybenzimidazole (PBI) Nanocomposite Membranes for Hydrogen Purification at High Temperatures. *Adv. Energy Mater.* **2012,** 2, 1358-1367.

(48) Villalobos, L. F.; Hilke, R.; Akhtar, F. H.; Peinemann, K. V. Fabrication of Polybenzimidazole/Palladium Nanoparticles Hollow Fiber Membranes for Hydrogen Purification. *Adv. Energy Mater.* **2017,** 8, 1701567.

(49) Zhu, L.; Swihart, M. T.; Lin, H. Tightening Polybenzimidazole (PBI) Nanostructure *via* Chemical Cross-Linking for Membrane H_2/CO_2 Separation. *J. Mater. Chem. A* **2017,** 5, 19914-19923.

(50) Yang, T. X.; Chung, T. S. Room-Temperature Synthesis of ZIF-90 Nanocrystals and the Derived Nano-Composite Membranes for Hydrogen Separation. *J. Mater. Chem. A* **2013,** 1, 6081-6090.

(51) Robeson, L. M. The Upper Bound Revisited. *J. Membr. Sci.* **2008,** 320, 390-400.

(52) Peng, Y.; Li, Y.; Ban, Y.; Yang, W. Two-Dimensional Metal-Organic Framework Nanosheets for Membrane-Based Gas Separation. *Angew. Chem. Int. Ed.* **2017,** 56, 9757-9761.

(53) Huang, A.; Liu, Q.; Wang, N.; Zhu, Y.; Caro, J. Bicontinuous Zeolitic Imidazolate Framework ZIF-8@GO Membrane with Enhanced Hydrogen Selectivity. *J. Am. Chem. Soc.* **2014,** 136, 14686-14689.